Life Sciences 357 (2024) 123059

Contents lists available at ScienceDirect

Life Sciences

journal homepage: www.elsevier.com/locate/lifescie

Unconventional p65/p52 NF-κB module regulates key tumor microenvironment-related genes in breast tumor-associated macrophages (TAMs)

Veronica De Paolis [a,*], Virginia Troisi [a], Antonella Bordin [b], Francesca Pagano [a], Viviana Caputo [c], Chiara Parisi [a,*]

[a] Institute of Biochemistry and Cell Biology, CNR-National Research Council, Via Ercole Ramarini, 32, 00015 Monterotondo Scalo, RM, Italy
[b] Department of Medical-Surgical Sciences and Biotechnologies, Sapienza University of Rome, Corso della Repubblica, 79, 04100, Latina, Italy
[c] Department of Experimental Medicine, Sapienza University of Rome, Viale Regina Elena, 324, 00161 Rome, Italy

ARTICLE INFO

Keywords:
Nuclear factor kappa-B (NF-κB)
Tumor-associated macrophages (TAMs)
Tumor microenvironment (TME)
Triple-negative breast cancer (TNBC)

ABSTRACT

The complex heterogeneity of tumor microenvironment (TME) of triple-negative breast cancer (TNBC) presents a significant obstacle to cytotoxic immune response and successful treatment, building up one of the most hostile oncological phenotypes. Among the most abundant TME components, tumor-associated macrophages (TAMs) have pivotal pro-tumoral functions, involving discordant roles for the nuclear factor kappa-B (NF-κB) transcription factors and directing to higher levels of pathway complexity.

In both resting macrophages and TAMs, we recently revealed the existence of the uncharacterized NF-κB p65/p52 dimer. In the present study, we demonstrated its enhanced active nuclear localization in TAMs and validated selected immune target genes as directly regulated by dimer binding on DNA sequences.

We demonstrated by ChIP-qPCR that p65/p52 enrichment on HSPG2 and CSF-1 regulatory regions is strictly dependent on macrophage polarization and tumor environment.

Our data provide novel mechanisms of transcriptional regulation in TAMs, orchestrated by the varied and dynamic nature of NF-κB combinations, which needs to be considered when targeting this pathway in cancer therapies.

Our results offer p65/p52, together with identified regulatory regions on genes impacting macrophage behavior and tumor biology, as novel molecular targets for TNBC, aimed at modulating TAMs functions towards anti-tumoral phenotypes and thus improving cancer treatment outcomes.

1. Introduction

Triple-negative breast cancer (TNBC) is the most hostile breast cancer (BC) subtype, lacking expression of estrogen receptor (ER), progesterone receptor (PR), and human epidermal growth factor receptor 2 (HER2), and representing a major cause of female mortality [1]. TNBC is a heterogeneous subgroup comprising about 10–15 % of breast cancer and exhibiting high levels of malignancy and invasiveness [1,2]. To date, the use of combined chemo- and immuno-therapy has enhanced treatment efficacy, although most patients develop primary or acquired resistance [2].

The tumor microenvironment (TME) of TNBC is extremely diversified [3], comprising cancer cells, tumor-associated macrophages (TAMs), soluble factors, and cancer-associated fibroblasts (CAFs), all embedded in the transformed extracellular matrix (ECM), with lower or absent $CD8^+$ T cells, playing a central role in antitumor immune response [4,5]. All TME components work dynamically to promote expansion of cancer cells by producing ECM, binding factors, and enzymatic modifiers [6]. In this complex scenario, TAMs, characterized by functional plasticity, can switch their polarization state and exhibit pro-tumoral or anti-tumoral functions. This cell population cannot be categorized into binary states like classically activated M1 or alternatively activated M2, but displays remarkable diversity and plasticity, leading to its classification into different subsets based on transcriptional landscape, functional properties, and cell surface markers [7]. Among them, M2-like subsets have critical roles in tumor progression by

* Corresponding authors.
E-mail addresses: veronica.depaolis@ibbc.cnr.it (V. De Paolis), chiara.parisi@cnr.it (C. Parisi).

https://doi.org/10.1016/j.lfs.2024.123059
Received 19 April 2024; Received in revised form 17 June 2024; Accepted 11 September 2024
Available online 13 September 2024

promoting angiogenesis, extracellular matrix remodeling, immune suppression, induction of Epithelial-Mesenchymal Transition (EMT), formation of pre-metastatic niches, and drug-resistance [8]. In TNBC, these subsets are determinants for cytotoxic T cell exclusion (immune desert phenotype) [9], so their high density correlates with a lower survival rate [10].

A growing number of studies focused on targeting both negative regulators of TAMs pro-tumoral activities, depleting macrophages or blocking their recruitment, and activator of TAMs antitumor efficacy, in order to reprogram them towards an anti-tumor phenotype or increase their phagocytic activity. Although some of these compounds are currently undergoing clinical trials for breast cancer, in combination with conventional chemotherapy or radiotherapy, gaining a deeper understanding to be translated into more effective strategies remains a challenge [11,12].

Multiple efforts to unravel the complexity of macrophages have highlighted key transcription factors (TFs) that orchestrate the reprogramming of TAMs. Among these, the nuclear factor kappa-light chain enhancer of activated B cells (NF-κB) family stands out as a master regulator of macrophage plasticity [13].

In vertebrates, the five NF-κB proteins (p50/NF-κB1, p52/NF-κB2, p65/RelA, RelB, and c-Rel) can form up to 15 distinct combinations of homo- or heterodimers, with 12 exhibiting the ability to bind DNA with either redundant or specific transcriptional activities [14–16]. Stimulation by various signals triggers the degradation of the inhibitory IκB proteins, resulting in the rapid nuclear translocation of NF-κB dimers [17]. Once in the nucleus, these dimers bind to specific DNA sequences known as κB sites, which are located within the regulatory regions of target genes [15,18]. Members of the Rel protein family (RelA, RelB, and c-Rel) possess the DNA binding transcriptional activation domain (TAD), allowing p50 and p52 subunits to form activating NF-κB dimers only when paired with Rel proteins [19]. The most common of these is the heterodimeric p65-p50 complex, a key effector of the canonical NF-κB activation pathway [20]. In contrast, the non-canonical pathway involves the phosphorylation and processing of NF-κB2/p100, which promotes the preferential formation of RelB-p52 heterodimer [21].

Many studies focused on the canonical NF-κB pathway and its constitutive activation is a commonly observed phenomenon in TNBC [22]. This pathway is crucial in the TME, playing a significant role in regulating tumor growth, survival, and resistance to therapy, and also enhancing the antitumor effects and immunosuppressive functions of different cells [23] and thus predicting the prognosis of breast cancer [24,25]. Instead, very little is known about the non-canonical pathway of NF-κB activation, although it predicts poor survival and resistance to therapy [26].

NF-κB is among the main regulators of TAMs function, playing essential and intricate roles in their polarization states. In fact, dysregulated NF-κB modules can both enhance macrophage polarization towards an M2-like phenotype, exacerbating pro-tumoral functions within the TME [13,23], or directly regulate the M1-like phenotype polarization, exerting tumor suppressor functions. In this direction, non-canonical RelB/p52 complexes are activated by autophagy in different cancer types, promoting TAMs M1 repolarization [27] while nuclear enrichment of the p50/p50 homodimers inhibits M1 activation by blocking the expression of inflammatory cytokines [28,29]. These apparently discordant activities suggest the existence of complex levels of NF-κB network organization.

In line with this idea, our recent findings have revealed the existence of a previously uncharacterized NF-κB p65/p52 interaction in nuclear extracts of macrophages and TAMs, suggesting that this dimer may play a role in DNA binding and transcriptional regulation [30].

In the present study, we further extended our findings, demonstrating the enhanced presence of active NF-κB p65/p52 signaling modules in TAMs and identifying target genes that are directly regulated by p65/p52 binding to specific regulatory sequences.

Our results shed light on the intricate interplay among NF-κB signaling pathways and TAMs plasticity, highlighting the dynamic nature of transcriptional regulation in response to external stimuli deriving from TME.

2. Materials and methods

2.1. Cell lines and treatments

Human breast cancer cell line MCF-7, human TNBC cell line MDA-MB-231, and human monocytic leukemia cell line THP-1 were obtained from ATCC. Cells were cultured in RPMI-1640 (Sigma-Aldrich, St. Louis, MO, USA) medium supplemented with 10 % fetal bovine serum (FBS) (Gibco, Waltham, MA, USA), 100 U/mL penicillin (Gibco), and 100 mg/mL streptomycin (Gibco) at 37 °C in a humidified incubator with 5 % CO_2.

Tumor-conditioned medium (TCM) was obtained from MDA-MB-231 and MCF-7 cancer cell lines as previously described [30]. MDA-MB-231 and MCF-7 were cultured in 10 % *v*/v FBS RPMI 1640 medium. Approximately 2×10^5 cells per mL were grown to 80 % of confluence, and the supernatants were harvested and centrifuged for 5 min at 500 ×*g* to remove suspended cells, then filtered (70 μm) and collected.

Undifferentiated macrophages were obtained by treating THP-1 cells (plated at a density of 3×10^5 cells per mL in a 6-well plate) with 100 ng/mL of the phorbol 12-myristate 12-acetate (PMA) (P8139; Sigma-Aldrich) for 24 h. Adherent THP-1 cells were left in fresh medium culture for 48 h before treatments.

Undifferentiated macrophages were maintained in Mφ state, M2-activated with IL-4 (20 ng/mL, 130–093-921; Miltenyi Biotec, Bergisch Gladbach, Germany), or polarized towards tumoral phenotype (TAM) with the addition of TCM (half of total volume) for 24 h or 48 h as previously described [30]. Undifferentiated macrophages were pre-activated to TAM phenotype for 16 h and then treated with 50 nM of N4-[2-(4-phenoxyphenyl)ethyl]-1,2-dihydroquinazoline-4,6-diamine (QNZ) (EVP4593, 481406; Calbiochem, San Diego, CA, USA) or dimethyl sulfoxide (DMSO) (Sigma-Aldrich) for 48 h.

2.2. Immunofluorescence analysis

M2 macrophages and TAMs were washed twice in PBS (Euroclone, Pero, Milan, Italy) and fixed in 4 % paraformaldehyde (PFA) for 20 min. Then, samples were blocked with 5 % of bovine serum albumin (BSA)-PBS + 0.3 % Triton X-100 (Sigma-Aldrich) for 1 h at RT and incubated overnight at 4 °C with primary human antibodies anti-p65 (1:50, D14E12; Cell Signaling Technology, Danvers, MA, USA) and anti-p52 (1:50, sc-7386; Santa Cruz Biotechnology, Dallas, Texas, USA) in 1 % BSA-PBS + 0.1 % Triton X-100. The secondary antibodies were diluted 1:200 in 1 % BSA-PBS and incubated for 2 h at RT: rabbit-Alexa Fluor 594 (A-11012, Invitrogen), mouse-Alexa Fluor 647 AffiniPure (715-605-150, Jackson, ImmunoResearch, Cambridge, UK). Nuclei were counterstained with DAPI (1:1,000, Sigma-Aldrich) for 10 min.

2.3. Image acquisition and processing

Confocal images were acquired by Olympus' PLAPON 60× OSC2 super-corrected objective lens. Sequential 0.3 μm thick *Z*-stacked sections were imaged through the entire sample and used to create maximum intensity projections (MIPs). All images of the same experiment were acquired with constant laser intensity and processed with Fiji (National Insitute of Health). Pearson's correlation coefficient (PCC) analysis was performed by Co-loc2 plugin-in of Fiji, with Costes threshold regression. Pearson's coefficient above a threshold higher than 0.3 in the nuclei was considered positive for colocalization of p65 and p52 proteins.

2.4. Gene expression analysis

Total RNA was isolated with TRizol (Invitrogen, Carlsbad, CA, USA), according to the manufacturer's protocol. RNA quantity was measured spectrophotometrically with the Nanodrop 100 System (Rockford, IL, USA). RNA (1 μg) was converted to cDNA by High-Capacity cDNA Reverse Transcription Kit (Applied Biosystem, Foster City, CA, USA) and quantitative real-time polymerase chain reaction (qRT-PCR) was carried out using the SensiFAST SYBR Hi-ROX Kit (Meridian Bioscience, Cincinnati, OH, USA). The fold change of each target gene was evaluated by ΔΔCt relative expression analysis. The primer sequences are provided in Table S1.

2.5. siRNA transfection

Undifferentiated macrophages (plated at a density of 3.5×10^5 cells in a 6-well plate) were transfected with 50 μM of siRNA (Horizon Discovery, Dharmacon, Lafayette, CO, USA) or 800 ng of esiRNA (Sigma-Aldrich). Transfection was performed in 1 mL of Opti-MEM Reduced Serum Media (Gibco) using 1.2 μL of Lipofectamine 2000 (Invitrogen), and after 5 h macrophages were polarized towards TAM phenotype. At the end of the established time point of 72 h, total protein lysate and RNA from each experimental condition were collected. The catalog number of each siRNA is provided in Table S2.

2.6. SDS-PAGE and western blots

TAMs were washed in PBS and lysed in RIPA buffer (50 mM Tris-HCl pH 7.5, 150 mM NaCl, 1 % Nonidet P-40, 0.5 % sodium deoxycholate, 0.1 % SDS, 1 mM EDTA) supplemented with 1 × Protease and Phosphatase Inhibitor Cocktail (PIC) (Sigma-Aldrich) for 30 min in ice and centrifugated for 15 min at 12,000 ×*g* at 4 °C. Protein concentration was evaluated with Bradford (Bio-Rad, Hercules, California, USA) protein assay against a standard of BSA. An equal amount of proteins (10 μg) were separated by SDS-PAGE and transferred onto nitrocellulose membranes (Amersham Biosciences, Amersham, UK). Membrane blocking was performed in TBS 0.01 % (*v/v*) Tween-20 (Sigma-Aldrich) with 5 % (*w/v*) non-fat dry milk (Applichem, Ottoweg, Darmstadt, Germany) for 1 h at RT. Primary antibodies were incubated overnight at 4 °C: anti-p65 (1:1,000, D14E12; Cell Signaling Technology), anti-p52 (1:100, sc-7386; Santa Cruz Biotechnology), anti-p50 (1:100, sc-8414; Santa Cruz Biotechnology), and anti-Vinculin (1:1,000, 4650; Cell Signaling Technology). Incubation of the membranes with HRP-conjugated anti-mouse (1:10,000, 315–035-003; Jackson, ImmunoResearch) or anti-rabbit (1:5,000, 111–035-144; Jackson, ImmunoResearch) was carried out at room temperature for 1 h. Chemiluminescence of protein bands was detected using the ECL Advance Western Blotting Detection Kit (Amersham Biosciences), acquired by ChemiDoc (Bio-Rad) instrument, and analyzed by densitometric analysis with the Fiji software.

2.7. Plasmids

Genomic human DNA was purified from THP-1 cells using the DNeasy Blood & Tissue kit (Qiagen, Valencia, CA). The HSPG2_R1-R4 and CSF-1_R1-R2 genomic regions (human hg38 version) were amplified by PCR using the High-Fidelity MyFi DNA polymerase (Meridian Bioscience). The primer sequences are provided in Table S3. PCR products were purified from agarose gel using the QIAquick Gel Extraction Kit (Qiagen) according to the manufacturer's instructions. Purified products were cloned in the pGL3-promoter vector (Promega, Madison, WI, USA) upstream of the SV40 promoter. The luciferase constructs obtained were used for the luciferase reporter assay. The pRL-TK vector (Promega) was used for the constitutive expression of wild-type Renilla luciferase, and the pGL3-basic vector (Promega) was used as a negative control.

2.8. Luciferase reporter assay

Undifferentiated macrophages (plated at a density of 1.5×10^5 in a 12-well culture plate) were cotransfected with luciferase constructs and pRL-TK vector. A ratio of 350 ng of total DNA to 0.7 μL of Lipofectamine 2000 (Invitrogen) in 0.5 mL of Opti-MEM Reduced Serum Media (Gibco) was used for each experimental condition. Macrophages were then polarized towards TAM phenotype and after 48 h luminescence was measured using Dual-Luciferase Reporter Assay (Promega) according to the manufacturer's protocol. The luciferase activity in transiently transfected TAMs was normalized to Renilla control and compared to empty pGL3-promoter vector.

2.9. ChIP-qPCR analysis

Chromatin cross-linking was performed with disuccinimidyl glutarate (DSG) and formaldehyde. 12×10^6 M2 macrophages and TAMs were fixed with 1.5 nM of DSG (Thermo Fisher Scientific, Waltham, Massachusetts, USA) for 45 min with gentle agitation at RT, and then with 1 % Formaldehyde (Sigma-Aldrich) for 12 min with gentle agitation at RT. Quenching was performed with 125 mM of Glycine for 5 min with gentle agitation at RT. M2 macrophages and TAMs were washed twice with PBS, harvested by gentle scraping in PBS, and pelleted for 5 min at 3,000 rpm at 4 °C. Fixed cells were lysed in 1 mL of Nuclei Lysis buffer (50 mM Tris-HCl pH 8.1, 10 mM EDTA, 1 % SDS) supplemented with 1× PIC for 10 min in ice, and then sonicated in a water bath sonicator (M220, Covaris, Woburn, Massachusetts, USA) to obtain fragments ranging from 200 to 400 bp, with the following setting: peak power:75.0; duty factor:10.0; cycle/burst:250; time: 900 s. Sheared chromatin was pelleted for 10 min at 14,000 rpm at 4 °C and then the supernatant was collected and diluted 10× in dilution buffer (16.7 mM Tris-HCl pH 8.1, 1.2 mM EDTA,167 mM NaCl, 0.01 % SDS, 1.1 % Triton X-100). Samples were pre-cleared to remove non-specific binding on beads with paramagnetic protein G beads (Invitrogen) for 2 h on a rotating platform at 4 °C. 1 % of the total volume was conserved as Input DNA, while collected samples were equally split and incubated on a rotating platform at 4 °C overnight with the following primary antibodies: anti-p65 (D14E12; Cell Signaling Technology), anti-p52 (sc-7386; Santa Cruz Biotechnology) and normal IgGs (12–370; MilliporeSigma) at a concentration of 1 μg per 1×10^6 cells. Samples were conjugated to paramagnetic protein G beads for 4 h on a rotating platform at 4 °C. Thereafter beads were sequentially washed for 5 min on a rotating platform at 4 °C with the following buffers: low salt (20 mM Tris-HCl pH 8, 150 mM NaCl, 2 mM EDTA pH 8, 1 % Triton X-100, 0.1 % SDS), high salt (20 mM Tris-HCl pH 8, 500 mM NaCl, 2 mM EDTA pH 8, 1 % Triton X-100, 0.1 % SDS), low salt, and twice in TE buffer (10 mM Tris-HCl pH 8, 1 mM EDTA pH 8). Beads and Input DNA were resuspended in elution buffer (10 mM Tris-HCl pH 8, 1 mM EDTA pH 8, 1 % SDS) and incubated overnight at 65 °C, with gentle agitation, and then ChIP samples were recovered from beads. ChIP and Input DNA were diluted 1:2 in TE buffer and reverse crosslinked with RNaseA (0.2 mg/mL) for 1 h at 37 °C following Proteinase K (0.2 mg/mL) incubation for 1 h at 55 °C. ChIP and Input DNA were purified with Phenol:Chloroform extraction (Ultrapure Phenol:Chloroform:Isoamyl Alcohol, Invitrogen) and ethanol precipitation. Samples were resuspended in 50 μL of Milli-Q water and qPCR was performed using SensiFAST SYBR Hi-ROX Kit. Data were normalized as a percent of the input method. The primer sequences are provided in Table S3.

2.10. Statistical analysis

GraphPad Prism 9 (La Jolla, California, USA) was used for statistical analysis. Data are presented as mean ± standard error of mean (SEM) from at least three independent experiments. The statistical significance was assessed by the one-way ANOVA with Tukey correction for gene expression analysis and unpaired two-tailed Student's *t*-test for

comparisons between two sets of data. p-values <0.05 (*), 0.01 (**), 0.001 (***), 0.0001 (****), ns: non-significant.

3. Results

3.1. Activation of the NF-κB p65/p52 signaling module in TAMs

A key indicator of the NF-κB signaling activation is the nuclear translocation of homo- or heterodimers of NF-κB subunits, which can form up to 15 possible combinations [14].

We previously showed the existence of atypical p65/p52 complexes in nuclear extracts from THP-1 derived macrophages and TAMs, and observed an enrichment of both subunits in the nucleic protein fractions of TAMs [30].

To clearly visualize their subcellular distribution in different polarization states, we now performed immunofluorescence/confocal microscopy analysis. A qualitative evaluation disclosed a more evident nuclear signal for both p65 and p52 in TAMs, compared to a primarily cytoplasmic distribution with mild nuclear localization in M2 macrophages (Fig. 1a). We further quantified the colocalization between nuclear p65 and p52 by calculating the Pearson's correlation coefficient (PCC). We observed a significant increase in the percentage of nuclei with positive p65 and p52 colocalization (cut-off of $r > 0.3$) in TAMs compared to M2 macrophages (Fig. 1b), with an average moderate index (PCC of $r > 0.5$) [31] (Fig. 1c).

These findings further prove the existence of a consistent p65/p52 nuclear association in TAMs, suggesting that these complexes are likely transcriptionally active.

3.2. Transcriptional modulation of p65/p52 target genes in TAMs

To investigate p65/p52-mediated gene regulation in TAMs, we checked for experimental available data on p65 and p52 co-occupancy in the "ChIP-Atlas: Peak Browser" database (https://chip-atlas.org/peak_browser) visualized on the IGV genome browser, restricting our search on regulatory regions of genes known to influence macrophage polarization, inhibition of macrophage recruitment to tumors, and immune checkpoint. This analysis generated a list of putative p65/p52 target genes (PTGs), including CSF-1, LILRB1, TNFAIP3, IL4R, TGFB1, CCL5, and HSPG2 (Fig. S1).

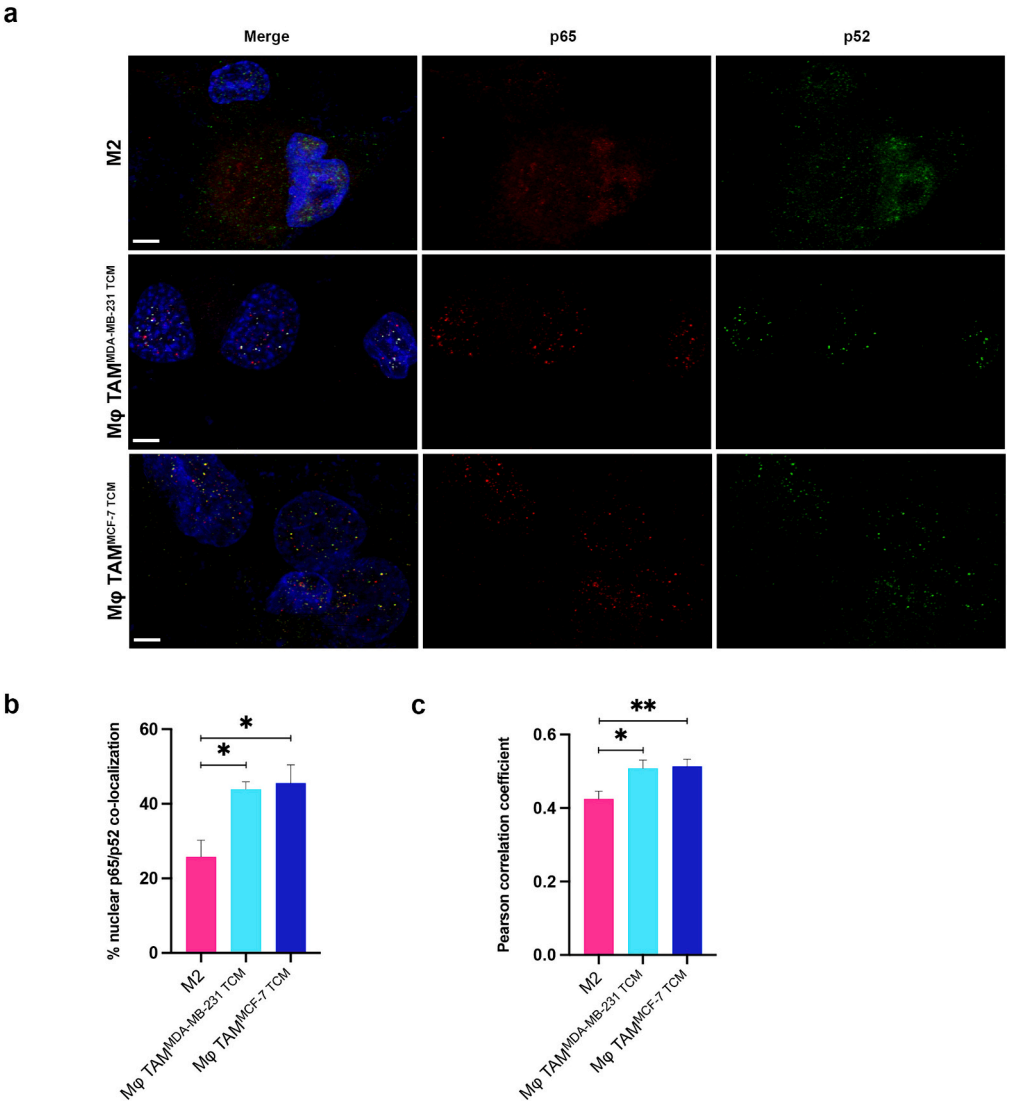

Fig. 1. p65/p52 nuclear colocalization. **a** Immunofluorescence analysis of p65 and p52 proteins in M2 macrophages, MφTAM$^{\text{MDA-MB-231 TCM}}$, and MφTAM$^{\text{MCF-7 TCM}}$ showing p65 in red, p52 in green, and colocalization dots in yellow. Nuclei were counterstained with DAPI. Scale bars represent 5 μm. **b** Quantitative p65 and p52 colocalization with Pearson's correlation coefficient (PCC) analysis using a cutoff of $r > 0.3$ to indicate positive colocalization. **c** Average Pearson's correlation coefficient. At least 90 cells were examined for each condition. Error bars represent ±SEM. Student's t-test was used to analyze the differences between M2 macrophages and TAMs; * $p < 0.05$, ** $p < 0.01$, $n = 3$ for each experimental groups.

Among the identified genes, CSF-1, TGFB1, and HSPG2 exhibited multiple regions for p65/p52 binding (Fig. S1 a-b-e).

Subsequently, we evaluated possible transcriptional changes of PTGs in untreated Mφ macrophages, M2 macrophages, and TAMs. Results unveiled a significant over-expression of CSF-1, LILRB1, and TNFAIP3 mRNA in both TAM subtypes, when compared to both Mφ and M2 macrophages. In contrast, we observed a moderate induction of IL4R in MφTAM$^{MCF\text{-}7\ TCM}$ compared to Mφ, and of CCL5 and TGFB1 compared to M2 macrophages (Fig. 2a).

We then asked whether the NF-κB family of TFs could be responsible for PTGs upregulation in TAMs. Thus, we assessed PTGs responsiveness to the general inhibitor of NF-κB transcriptional activation N4-[2-(4-

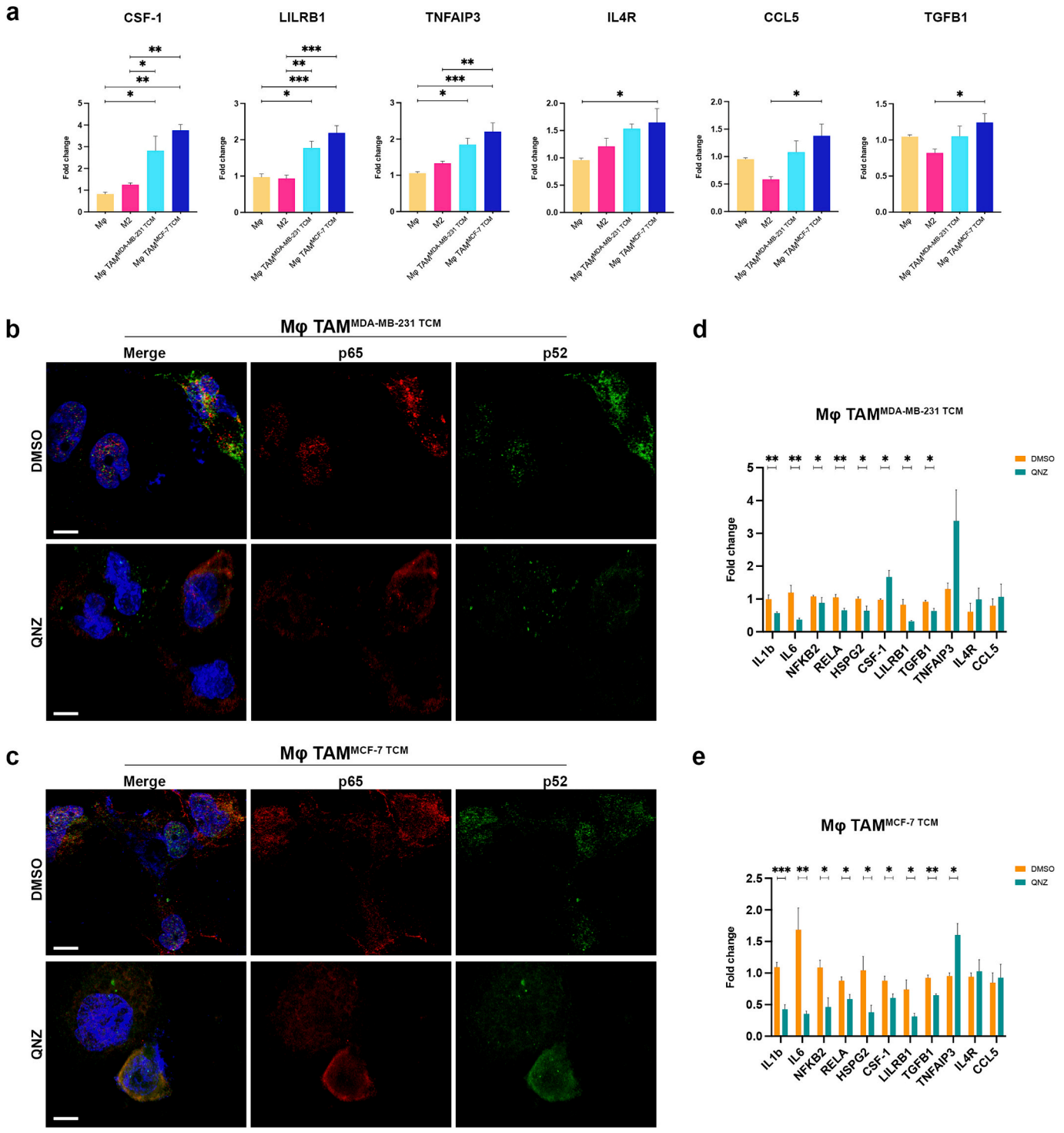

Fig. 2. p65/p52 putative target genes (PTGs). **a** Gene expression analysis of PTGs was evaluated in untreated and treated macrophages by qRT-PCR. Error bars represent ±SEM. One-way ANOVA and Tukey correction were used to evaluate the differences between means; * $p < 0.05$, ** $p < 0.01$, *** $p < 0.001$. $n = 4$ for each experimental group. Immunofluorescence analysis of p65 and p52 proteins in **b** MφTAM$^{MDA\text{-}MB\text{-}231\ TCM}$ and **c** MφTAM$^{MCF\text{-}7\ TCM}$ treated with QNZ, compared to control DMSO. p65 was stained in red and p52 in green. Nuclei were counterstained with DAPI. Scale bars represent 5 μm. Gene expression analysis of NF-κB PTGs by qRT-PCR in **d** MφTAM$^{MDA\text{-}MB\text{-}231\ TCM}$ and **e** MφTAM$^{MCF\text{-}7\ TCM}$ treated with QNZ, compared to control DMSO. Error bars represent ±SEM. Student's *t*-test was used to analyze the efficacy of QNZ treatment for each gene, compared to the control treatment; * $p < 0.05$, ** $p < 0.01$, *** $p < 0.001$. $n = 3$ for each experimental group.

phenoxyphenyl)ethyl]-1,2-dihydroquinazoline-4,6-diamine (QNZ). Immunofluorescence analysis confirmed that QNZ was able to prevent the nuclear translocation of both p65 and p52 subunits, compared to control DMSO treatment (Fig. 2b–c). Gene expression analysis (Fig. 2d–e) showed significant downregulation of LILRB1 and TGFB1 mRNA in QNZ-treated TAMs, compared to those treated with DMSO, along with downregulation of known NF-κB target genes (IL-6, IL-1b, RELA (p65), NF-κB2 (p52), and HSPG2 [30,32]). Surprisingly, CSF-1 showed differential transcriptional modulation in response to QNZ in different TAMs subtypes, as we observed CSF-1 mRNA upregulation in treated MφTAM$^{MDA\text{-}MB-231\ TCM}$ (Fig. 2d), and downregulation in MφTAM$^{MCF\text{-}7\ TCM}$ (Fig. 2e). Additionally, TNFAIP3 was significantly upregulated in MφTAM$^{MCF\text{-}7\ TCM}$ upon NF-κB inhibition.

Thus, among genes of PTGs list, our results confirmed CSF-1, LILRB1, TGFB1, and HSPG2 as TAM activated and NF-κB target genes (TGs), to be further investigated for specific p65/p52 regulation.

3.3. Exclusion of p50 subunit involvement in the regulation of most selected TGs in TAMs

P50 is the most common heterodimerization partner of p65 in the canonical NF-κB signaling pathway, principally culminating in upregulating gene expression, and whose activation is widely observed in TNBC [22]. However, p50 can also form homodimers with inhibitory effects [33].

To inquire about p50 subunit involvement in transcriptional changes observed in TAMs, we analyzed CSF-1, LILRB1, TGFB1, and HSPG2 mRNA levels following the silencing of p50. Western blot analysis on total protein extracts confirmed a significant reduction of p50 protein levels in both MφTAM$^{MDA\text{-}MB-231\ TCM}$ and MφTAM$^{MCF\text{-}7\ TCM}$ (Fig. 3a–b). In these conditions, no significant variation was observed for the mRNA expression of all the analyzed targets in MφTAM$^{MDA\text{-}MB-231\ TCM}$ (Fig. 3c) while significant changes were observed only for TGFB1 and CSF-1 in MφTAM$^{MCF\text{-}7\ TCM}$ (Fig. 3d). In particular, the reduction of p50 downregulated TGFB1 and upregulated CSF-1 mRNAs in MφTAM$^{MCF\text{-}7\ TCM}$, indicating positive and negative regulatory actions on these genes, respectively.

These results suggest that neither the canonical p65/p50 heterodimer nor the inhibitory p50/p50 homodimer is involved in the regulation of the selected TGs in MφTAM$^{MDA\text{-}MB-231\ TCM}$. Instead, they highlight dynamic interactions involving p50 on TGFB1 and CSF1 promoters in MφTAM$^{MCF\text{-}7\ TCM}$.

3.4. Differential regulation of TGs by p65 and p52 in breast cancer environments

Based on the results obtained from p50 silencing, we inquired if p65 and p52 could be the main NF-κB actors involved in the transcriptional regulation of TGs. Thus, we downregulated p65 or p52 protein in both TAMs using siRNAs. As shown in Fig. 4a–b, western-blot analysis confirmed a consistent and specific reduction of each subunit of the complex in TAMs, as silencing of p65 didn't affect p52 protein levels, and *vice versa*. Both p65 and p52 silencing produced a significant downregulation of CSF-1, LILRB1, TGFB1, and HSPG2 mRNA in MφTAM$^{MDA\text{-}MB-231\ TCM}$ (Fig. 4c), while a similar effect was observed only for CSF-1 and LILRB1 mRNA in MφTAM$^{MCF\text{-}7\ TCM}$ (Fig. 4d). On the other hand, in MφTAM$^{MCF\text{-}7\ TCM}$, we observed a significant downregulation of TGFB1 mRNA only in p65 silenced MφTAM$^{MCF\text{-}7\ TCM}$, and no significant

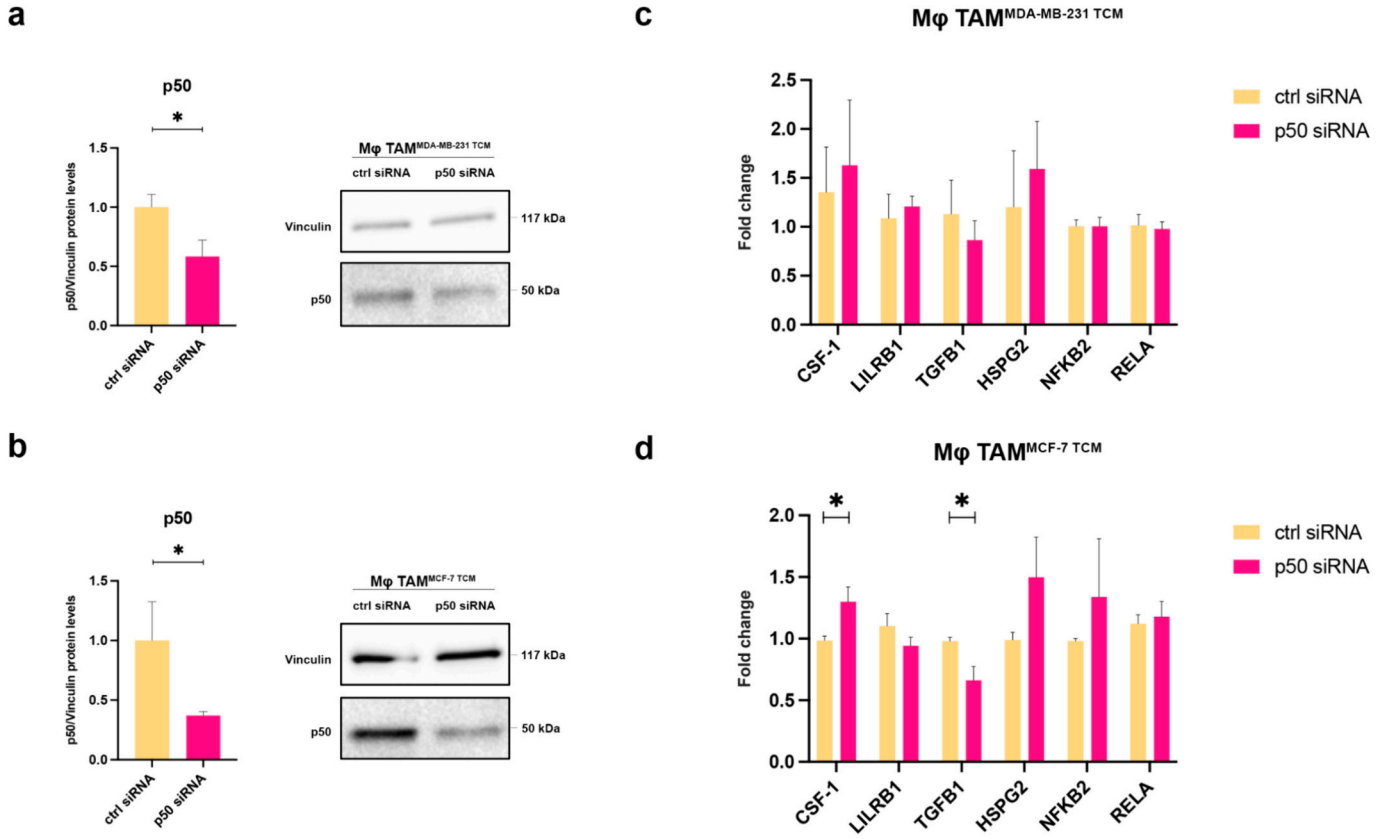

Fig. 3. p50 downregulation in TAMs. Western blot analysis of p50 protein was performed in **a** MφTAM$^{MDA\text{-}MB-231\ TCM}$ and **b** MφTAM$^{MCF\text{-}7\ TCM}$ transfected with p50 siRNA, compared to control siRNA (ctrl siRNA). P50 protein level was normalized on the Vinculin protein level. Error bars represent ±SEM. Student's *t*-test; * $p < 0.05$. $n = 4$ for each experimental group. Gene expression analysis of TGs was evaluated by qRT-PCR in **c** MφTAM$^{MDA\text{-}MB-231\ TCM}$ and **d** MφTAM$^{MCF\text{-}7\ TCM}$ transfected with p50 siRNA, compared to control siRNA. Error bars represent ±SEM. Student's t-test was used to analyze the mRNA level of each gene after p50 downregulation, compared to control siRNA; * $p < 0.05$. $n = 4$ for each experimental group.

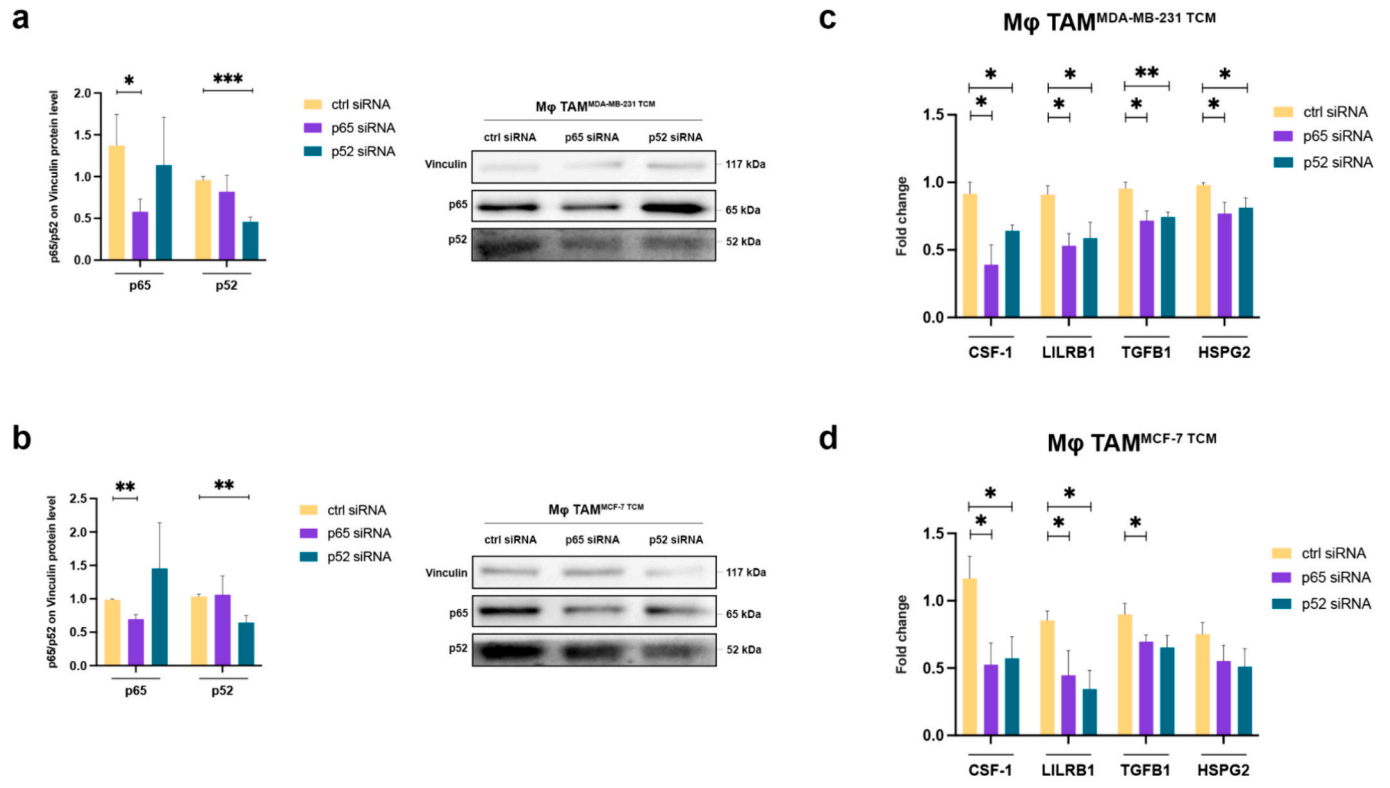

Fig. 4. p65 and p52 downregulation in TAMs. Western blot analysis of p65 and p52 protein was performed in **a** MφTAM$^{MDA\text{-}MB-231\ TCM}$ and **b** MφTAM$^{MCF\text{-}7\ TCM}$ transfected with p65 and p52 siRNA, compared to control siRNA (ctrl siRNA). P65 and p52 protein levels were normalized on the Vinculin protein level. Error bars represent ±SEM. Student's *t*-test was used to analyze p65 or p52 silencing efficacy compared to control siRNA; * $p < 0.05$, ** $p < 0.01$, *** $p < 0.001$. $n = 5$ for each experimental group; $n = 4$ for p52 MφTAM$^{MDA\text{-}MB-231\ TCM}$. Gene expression analysis of TGs was evaluated by qRT-PCR in **c** MφTAM$^{MDA\text{-}MB-231\ TCM}$ and **d** MφTAM$^{MCF\text{-}7\ TCM}$ transfected with p65 and p52 siRNA, compared to control siRNA. Error bars represent ±SEM. Student's t-test was used to analyze the mRNA level of each gene after p65 or p52 downregulation, compared to control siRNA; *$p < 0.05$, **$p < 0.01$. $n = 5$ for each experimental group.

variation of HSPG2 mRNA was observed in MφTAM$^{MCF\text{-}7\ TCM}$ after both p65 and p52 silencing (Fig. 4d).

These findings indicate that both p65 and p52 cooperate in regulating the selected TGs in MφTAM$^{MDA\text{-}MB-231\ TCM}$. However, the specific regulation of TGFB1 by p65 and its previously observed modulation by p50 suggest that canonical NF-κB signaling predominantly governs its expression in MφTAM$^{MCF\text{-}7\ TCM}$.

3.5. *Expanding p65/p52 binding site analysis on HSPG2 and CSF-1 regulatory regions*

We then asked if transcriptional regulation of TGs occurred through direct binding of p65/p52 to their regulatory regions, or by indirect regulation of a common downstream target gene.

To address this, we extended our *in silico* analysis of p65/p52 binding to specific regulatory elements of the HSPG2, CSF-1, TGFB1, and LILRB1 genes. Using the UCSC Genome Browser Database (https://genome.ucsc.edu) we included ENCODE annotation data [34] identifying p65/p52 peaks in annotated promoter and enhancer regions. These regions are characterized by DNase I Hypersensitivity peaks and histone modifications, as H3K4Me3, H3K4Me1, and H3K27Ac marks. Additionally, we used the "JASPAR Transcription Factor Binding site database" [35] and the "ReMap Atlas of Regulatory Regions" [36], to analyze both predicted and validated transcription factor binding sites through functional assays.

Compared to our previous analysis, based on the "ChIP-Atlas: Peak Browser" database (Fig. S1e), we identified some additional p65/p52 binding regions. As shown in Fig. 5a, when looking at p65 (RELA) and p52 (NFKB2) binding sites on HSPG2 regulatory elements, we found three different regions with overlapping or very closed RELA and NFKB2 peaks (HSPG2_R1–3-4), and one harboring only RELA binding site (HSPG2_R2) which had been already validated *in vitro* for its activity in transcription of HSPG2 in prostate cancer cells [37]. The identified regions reside in distinct regulatory areas, as shown in the ReMap density panel. HSPG2_R1 is located in an upstream enhancer (chr1:21,957,107-21,957,409); HSPG2_R2-R3 in a promoter region upstream and downstream the TSS (chr1:21,939,575:21,939,823 and chr1:21,927,522-21,927,704, respectively); HSPG2_R4 is located in the first intron, in a downstream enhancer (chr1:21,909,534-21,909,930).

We generated constructs able to assess differences in promoter activity by inserting the above identified sequences upstream of the CMV promoter in a luciferase reporter pGL3 vector.

Results disclosed that HSPG2_R3 and R4 significantly increases luciferase activity, with a distinct pattern of activation between M2 macrophages and TAMs. In particular, HSPG2_R3 specifically enhanced promoter activity in M2 macrophages, while HSPG2_R4 in both TAMs, compared to control vector (Fig. 5b).

To confirm the direct p65/p52 binding on HSPG2_R3 and HSPG2_R4 regions in M2 macrophages and TAMs, we performed ChIP-qPCR assays.

P65 possesses a transactivation domain and binds the DNA elements, while p52 does not [19]. Sheared chromatin was then immunoprecipitated with p65 and p52 antibodies, along with control IgG, following an adapted two-step cross-linking (see Material and Methods), and qPCR analysis was performed to detect the predicted p65/p52 binding sequences. The amplification of p65 and p52 positive (NFKIB) and negative (alpha-satellite) targets (Fig. S2a–b), was assessed to verify the specific p65 and p52 enrichment, compared to control IgG. Results showed that p65 binds the HSPG2_R3 region in M2 macrophages and the HSPG2_R4 region in MφTAM$^{MDA\text{-}MB-231\ TCM}$ (Fig. 5c). Furthermore, p52 enrichment showed a similar behavior with significant enrichment in

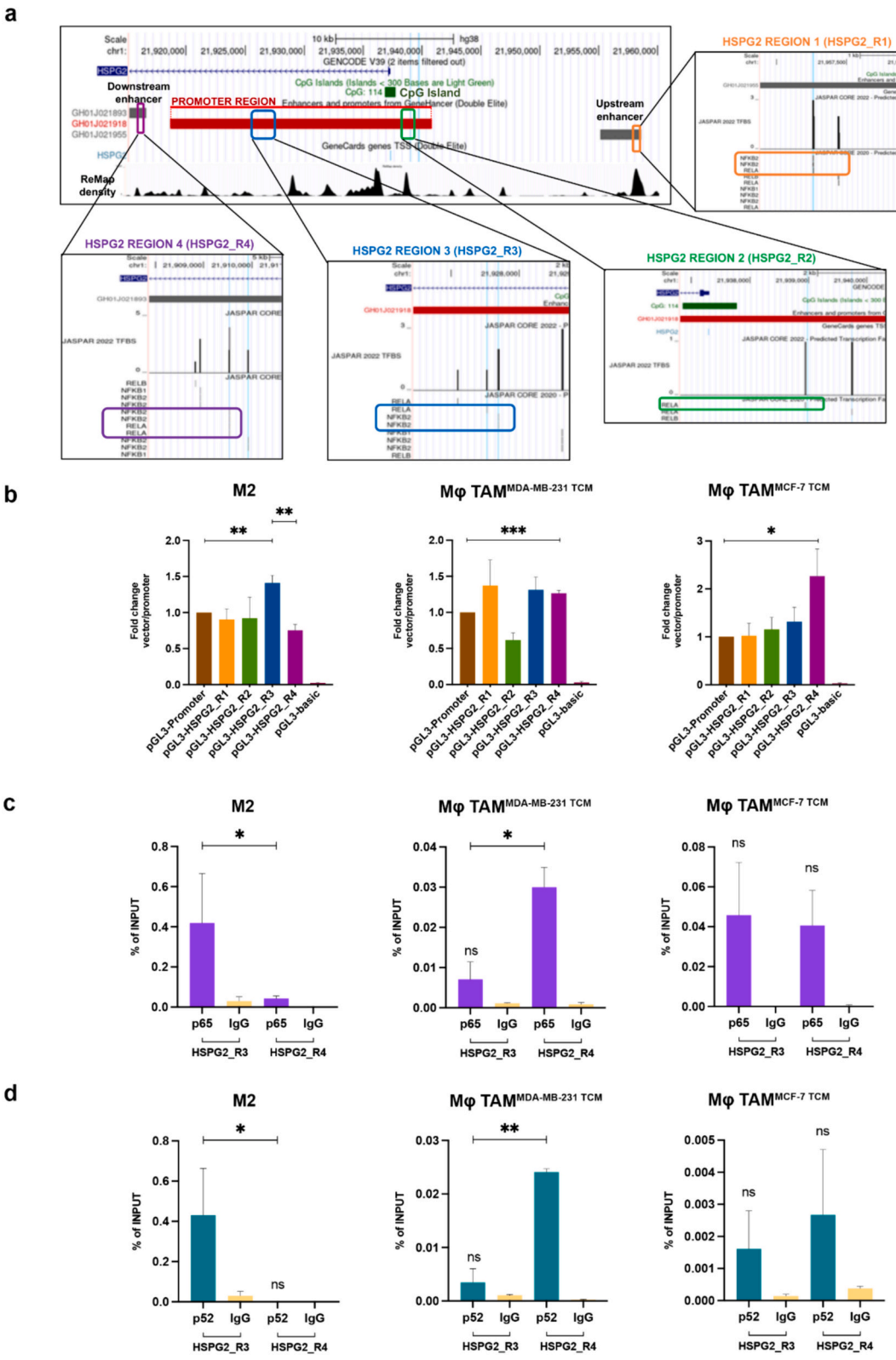

Fig. 5. HSPG2 regulatory elements. **a** *In silico* analysis of HSPG2 on the UCSC Genome Browser showed four regulatory regions with RELA (p65) and NFKB2 (p52) binding sites, as shown in the lower panel (JASPAR 2022 TFBS and ReMap density tracks). **b** The luciferase assay of the HSPG2 regulatory regions was performed in M2 macrophages and TAMs. Data represents firefly/renilla luminescence. Error bars represent ±SEM. Student's *t*-test: $*p < 0.05$, $**p < 0.01$, $***p < 0.001$. $n = 4$ for each experimental group. ChIP-qPCR analysis of **c** p65 and **d** p52 was performed in M2 macrophages and TAMs on HSPG2_R3 and HSPG2_R4 regulatory regions. Quantitative PCR data is presented as a percentage of the input chromatin control, compared to control IgG. Student's t-test was performed to compare the antibody enrichment to IgG. ns = not significant enrichment of antibody compared to control IgG; $*p < 0.05$ were none reported. Student's t-test was also performed to compare the antibody enrichment between the two regulatory regions: $*p < 0.05$, $**p < 0.01$, $***p < 0.001$. $n = 4$ for each experimental group.

the HSPG2_R3 region in M2 macrophages and in HSPG2_R4 in MφTAM$^{MDA\text{-}MB-231\ TCM}$(Fig. 5d). Consistent with previous results from p65 and p52 silencing, no significant enrichment of both p65 and p52 was observed in MφTAM$^{MCF\text{-}7\ TCM}$ for both analyzed HSPG2 regions (Fig. 5c–d).

For the CSF-1 regulatory elements, our *in silico* analysis identified two distinct regions (CSF-1_R1 and CSF-1_R2) within the promoter, both containing overlapping p65 and p52 binding sites. Both regions reside upstream of TSS (chr1:109,910,324-109,910,608 and chr1:109,910,606-109,910,955) in a high density ReMap area (Fig. 6a). Luciferase assay showed differential promoter activities in TAMs in the presence of two regions, while no significant variation was observed in M2 macrophages (Fig. 6b). Specifically, CSF-1_R2 enhanced promoter activity in MφTAM$^{MDA\text{-}MB-231\ TCM}$, whereas CSF-1_R1 was actively enhancing the reporter gene transcription in MφTAM$^{MCF\text{-}7\ TCM}$, suggesting a fine CSF-1 transcriptional regulation. We performed ChIP-qPCR analysis of p65 and p52 binding to these regulatory regions, finding that both proteins bind CSF-1_R2 in MφTAM$^{MDA\text{-}MB-231\ TCM}$ and CSF-1_R1 in MφTAM$^{MCF\text{-}7\ TCM}$ (Fig. 6c–d). Differently, in M2 macrophages p65 bound to both CSF-1 regulatory regions (Fig. 6c), while p52 showed no significant enrichment (Fig. 6d).

3.6. Analysis of p65/p52 binding on regulatory regions of TGFB1, and LILRB1

When looking at TGFB1 locus we similarly found two p65/p52 binding sites, one nearby of the TSS (TGFB1_R1, chr19:41,353,746-41,353,895) and another in the first intron (TGFB1_R2, chr19:41,351,420-41,351,617).

ChIP-qPCR analysis performed on these regions demonstrated p65 enrichment at TGFB1_R2 in both M2 macrophages and TAMs (Fig. 7a), with no significant enrichment of p52 observed (Fig. 7b).

For LILRB1, a single p65/p52 binding site was identified in the first intron (chr19:54,616,876-54,617,208) (Fig. S1d). ChIP-qPCR analysis revealed significant p65 enrichment (Fig. 7c) in this regulatory region for both M2 macrophages and TAMs, whereas p52 (Fig. 7d) did not show significant binding.

4. Discussion

TAMs are key components of the intricate interplay between cancer cells and the immune system. Understanding their crosstalk within the TME is becoming crucial to develop targeted therapies that can disrupt pro-tumoral signaling and promote anti-tumor immune responses.

NF-κB pathways are among the main determinants of TAMs polarization states [13,23] and also recognized actors of tumor initiation and progression.

Given this evidence, a large number of global NF-κB inhibitors have been developed and some have entered clinical trials. The principal reason for their limited efficacy is often due to their severe dose-limiting toxicities, caused by the lack of selectivity in inhibiting NF-κB pathogenic activity without disrupting its essential physiological functions.

One challenge is that most of the research has always paid attention to known NF-κB pathways, principally the canonical (p65/p50) [25] and less extensively the non-canonical one (p52/RelB) [38], thereby missing some levels of pathway complexity.

Moreover, a strategy to selectively target NF-κB pro-tumoral activity in TAMs has never been explored.

We recently demonstrated the existence of a previously unexplored NF-κB p65/p52 dimerization in nuclear extract of BC associated TAMs [30]. It is well known that nuclear accumulation is a crucial event for NF-κB dimers activation, as it enables their access to DNA and consequent transcriptional modulation.

In this study, we aimed to characterize p65/p52 subcellular distribution, by the means of immunofluorescence and colocalization studies. We were able to further demonstrate the presence of colocalization spots indicative of active nuclear p65/p52 dimers in macrophages. Additionally, we revealed increased dimers accumulation in nuclei of TAMs associated with TNBC (MφTAM$^{MDA\text{-}MB-231\ TCM}$) and adenocarcinoma BC (MφTAM$^{MCF\text{-}7\ TCM}$), compared to M2 differentiation state. This suggests that exposure to the tumoral secretome triggers the activation of the NF-κB p65/p52 signaling module.

Consequently, we hypothesized that the heightened NF-κB p65/p52 activation in TAMs could play a role in shaping their distinct transcriptomic profiles, thereby influencing their unique functional properties and behaviors of TAMs in the context of cancer progression.

So we focused on genes known to be involved in the processes of TAM polarization, immune escape, and acquired drug resistance, all specific hallmarks of TNBC [39]. Using an *in silico* approach, we identified genes with overlapping p65 and p52 binding sequences within their regulatory regions. This analysis pinpointed CSF-1, LILRB1, TNFAIP3, IL4R, TGFB1, CCL5, and HSPG2 genes as candidate genes for p65/p52 transcriptional regulation (PTGs).

In support of this hypothesis and consistent with our previous findings on HSPG2 [30], CSF-1, LILRB1, and TNFAIP3 mRNA levels showed upregulation in TAMs exposed to both TNBC and BC environments, concomitant to p65/p52 nuclear enrichment, while a milder induction was also observed for IL4R, CCL5 and TGFB1 in MφTAM$^{MCF\text{-}7\ TCM}$. However, when assessing gene responsiveness to the general NF-κB inhibitor QNZ in TAMs, only LILRB1, TGFB1, and CSF-1 were confirmed as novel NF-κB targets, similar to HSPG2 [30] and to the already known IL1b, IL6, NFKB2 (p52) and RELA (p65) target genes [32].

The new candidates genes play distinct and prominent roles in TAMs/tumor crosstalk. Specifically, heparan sulfate proteoglycan 2 (HSPG2) is one of the most represented tECM molecules that sequester proteins, growth factors, cytokines, and enzymes *via* its attached heparan sulfate (HS) chain [40]. Our previous data on TNBC biopsies showed a distinctive stromal deposition of HSPG2 by TAMs in high cell density areas and surrounding tumor islands where TAMs are highly infiltrated [30], mimicking a physical shield that could exclude $CD8^+$ T cell and thus representing a molecular link between ECM regulation by NF-κB in TAMs. On the other hand, CSF-1 is involved in macrophage recruitment, differentiation, and polarization towards M2-like TAMs [41] while LILRB1 is associated with the inhibition of phagocytosis of cancer cells, binding the tumoral HLAI, acting as a myeloid checkpoint [42]. Of note, both CSF-1 and LILRB1 have been exploited as promising targets for myeloid cell reprogramming in pre-clinical and clinical trials [12]. Finally, TGF-β is involved in ECM remodeling, pathological fibrosis, and immunosuppression by promoting the expansion of regulatory T cells [43].

Among the candidate genes, CSF-1 showed peculiar NF-κB responsiveness, that varied depending on the BC environment. This specific hallmark points to a finely context-dependent nature of NF-κB pathway activity and its downstream effects on gene expression, in line with the dynamic and adaptable nature of TAMs in response to their microenvironment [7].

Unfortunately, the extracellular signaling molecules leading to the formation of atypical p65/p52 dimer remains unknown. Our data suggest taking in consideration possible feedback interplay among regulated ECM related proteins such as HSPG2 and TGF-β and differential NF-κB TFs dimerization.

Supporting the idea of a dynamic dimer composition, we demonstrated a distinct pattern of NF-κB members' contributions to the transcriptional regulation of TGs associated to different cancer secretomes.

By performing independent and selective subunit silencing, we found that p65 and p52 proteins were major contributors to the transcriptional changes of all selected targets in MφTAM$^{MDA\text{-}MB-231\ TCM}$. Additionally, luciferase assays and ChIP analysis specifically mapped p65 and p52 binding sites on the analyzed (HSPG2_R4 and CSF-1_R2) regulatory regions, thus corroborating a predominant and direct role for p65/p52 module activation at least for these genes.

Conversely, in MφTAM$^{MCF\text{-}7\ TCM}$ we observed a more complex NF-κB

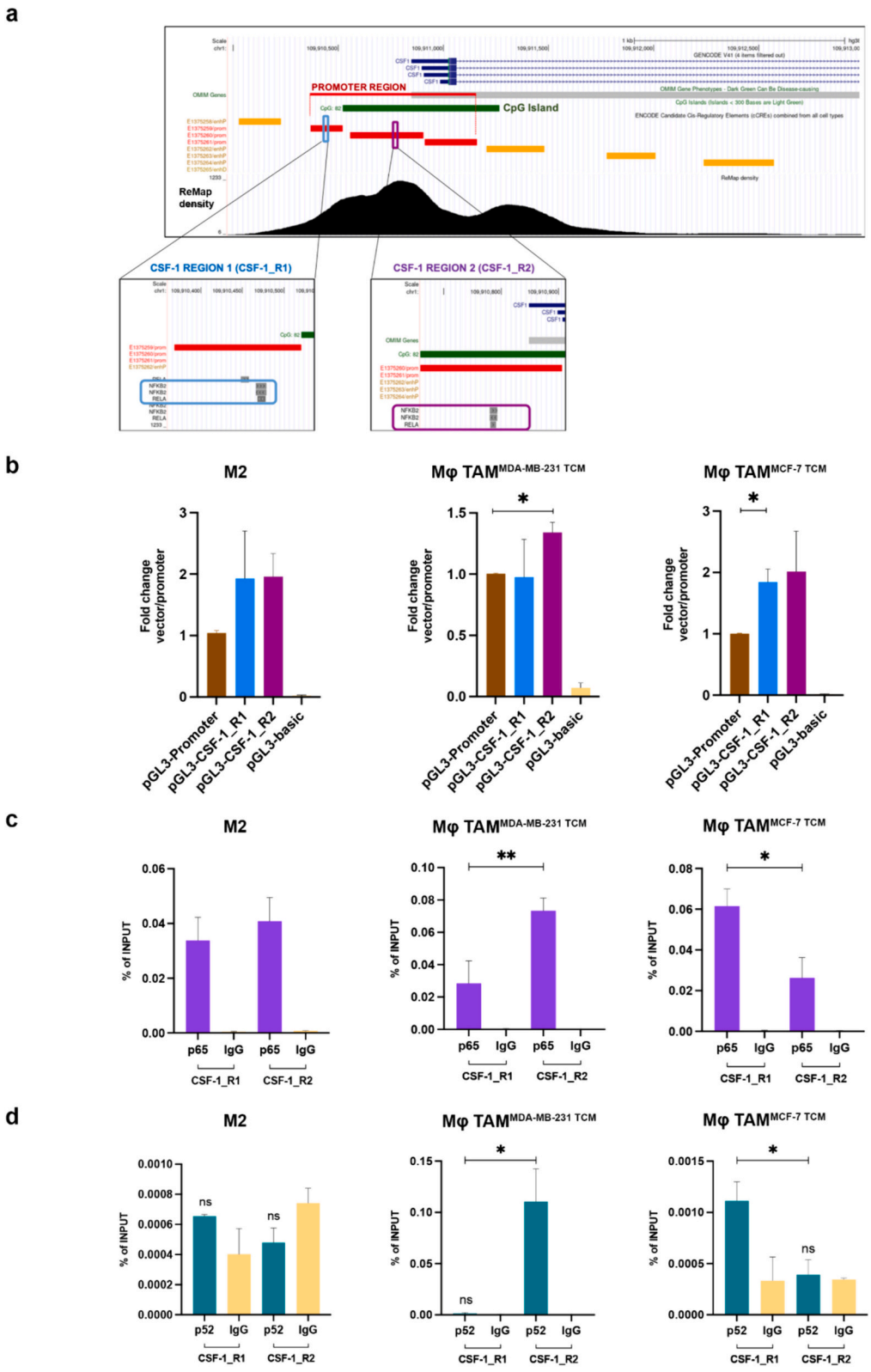

Fig. 6. CSF-1 regulatory elements. **a** *In silico* analysis of CSF-1 on the UCSC Genome Browser showed two regulatory regions with overlapped RELA (p65) and NFKB2 (p52) binding sites, as shown in the lower panel (JASPAR 2022 TFBS and ReMap density tracks). **b** The luciferase assay of the two CSF-1 regulatory regions was performed in M2 macrophages and TAMs. Data represents firefly/renilla luminescence. Error bars represent ±SEM. Student's *t*-test: $*p < 0.05$. $n = 4$ for each experimental group. ChIP-qPCR analysis of **c** p65 and **d** p52 was performed in M2 macrophages and TAMs on CSF-1_R1 and CSF-1_R2 regulatory regions. Quantitative PCR data is presented as a percentage of the input chromatin control, compared to control IgG. Student's t-test was performed to compare the antibody enrichment to IgG. ns = not significant enrichment of antibody compared to control IgG; *p < 0.05 were none reported. Student's t-test was also performed to compare the antibody enrichment on the two regulatory regions: $*p < 0.05$, $**p < 0.01$. $n = 4$ for each experimental group.

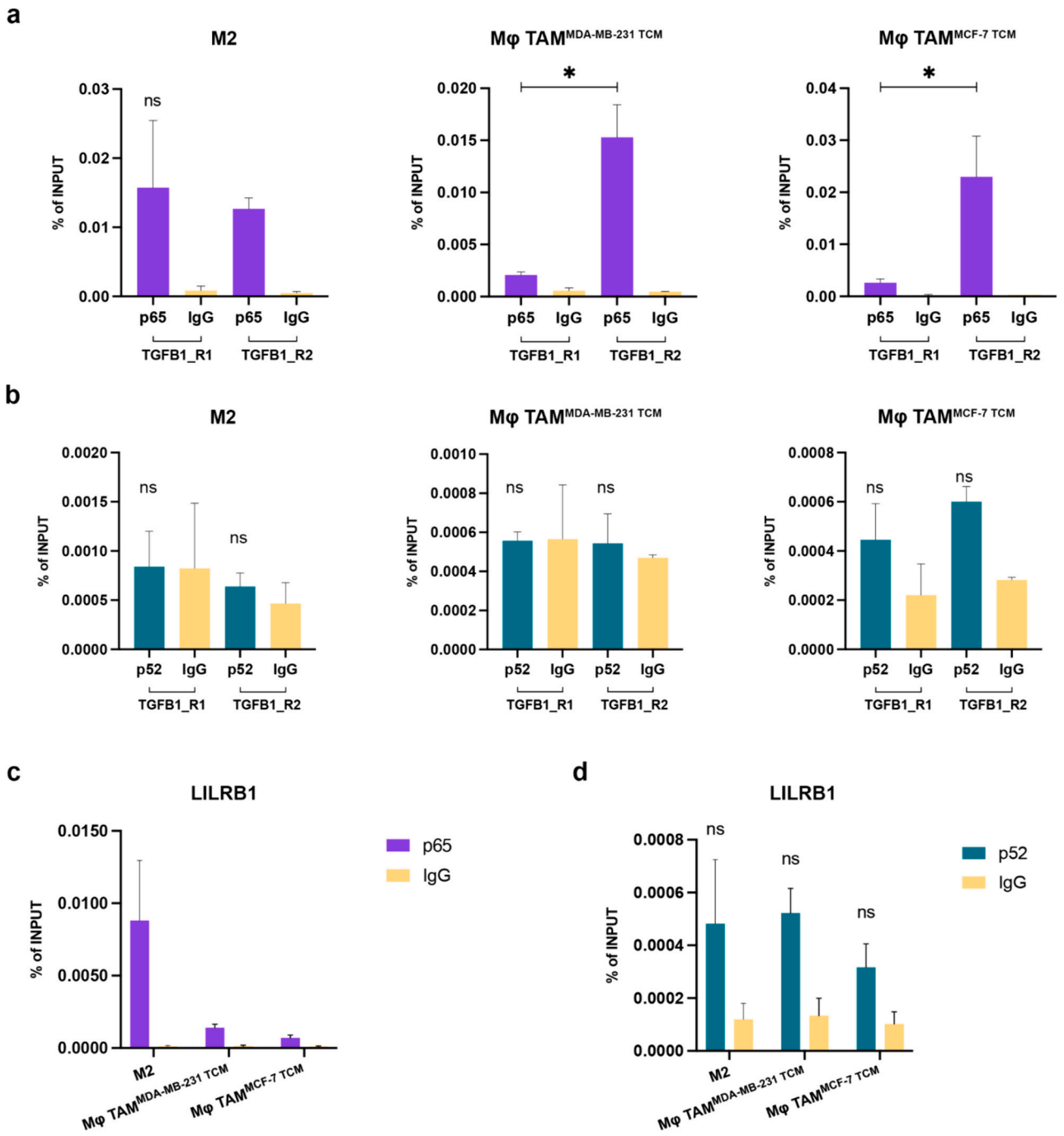

Fig. 7. TGFB1 and LILRB1 regulatory elements. ChIP-qPCR analysis of **a** p65 and **b** p52 was performed in M2 macrophages and TAMs on TGFB1_R1 and TGFB1_R2 regulatory regions. Quantitative PCR data is presented as a percentage of the input chromatin control, compared to control IgG. $n = 3$ for each experimental group. ChIP-qPCR analysis of **c** p65 and **d** p52 was performed in M2 macrophages and TAMs on the LILRB1 p65/p52 binding site. Quantitative PCR data is presented as a percentage of the input chromatin control, compared to control IgG. $n = 3$ for each experimental group. Student's *t*-test was performed to compare the antibody enrichment to IgG. ns = not significant enrichment of antibody compared to control IgG; $*p < 0.05$ were none reported. Student's t-test was also performed to compare the antibody enrichment on the regulatory region: $*p < 0.05$, $**p < 0.01$.

activity. Specifically, TGFB1 regulation predominantly depended on p65 and p50, indicating a reliance on canonical signaling. More compellingly, CSF-1 showed both positive regulation by p65 and p52, and negative regulation by p50. This dual regulation suggests the involvement of both the activating p65/p52 module and the inhibitory p50/p50 dimer [33].

Finally, HSPG2 expression resulted to be independent of selected NF-κB members in MφTAM$^{MCF\text{-}7\ TCM}$, suggesting other regulatory mechanisms or transcription factors downstream of the NF-κB signaling pathway playing more direct roles in its modulation.

In line with these results, no specific enrichment was found for p65 or p52 by ChIP in the HSPG2 regulatory regions in MφTAM$^{MCF\text{-}7\ TCM}$.

These data, together with the differential enrichment of p65/p52 on HSPG2_R3 only in M2 macrophages, demonstrate that activation of distinct regulatory regions is strictly dependent on cell polarization state and on the pathological context driving it, allowing a fine-tuned HSPG2 transcriptional regulation.

This can be easily extended at least to CSF-1 gene regulation. In fact,

our luciferase reporter and ChIP data showed exclusive activation of CSF-1_R1 with p65/p52 enrichment in MφTAM$^{MCF\text{-}7\ TCM}$ while the same effect was selective for CSF1_R2 in MφTAM$^{MDA\text{-}MB-231\ TCM}$ and any region showed significant effects in M2 macrophages.

Our data highlight a new role for NF-κB p65/p52 in orchestrating pro-tumoral mechanisms within TAMs. Developing novel tools that specifically target the p65/p52 complex, which regulates several targetable genes TAMs, could enhance the efficacy of current therapy.

The proven existence of active alternate p65/p52 dimers provides a crucial link between the canonical and non-canonical NF-κB pathways, allowing for the integration of signals from the TME and deeply defining the regulation of genes involved in tumor progression. Our results point out a more complex interplay among NF-κB family members in TAMs, indicating a continuum between canonical and non-canonical pathways states, strictly dependent on specific gene context and external signals. Although there are still limited studies on this topic, challenging pieces of evidence exist and are indeed in line with this observation. Consistent with our case, the alternate p65/p52 dimer has been shown to form upon lymphotoxin b receptor (LTbR)-activated non-canonical signaling to prolong the canonical response to Toll-like receptor 4 (TLR4) in mouse fibroblasts and intestinal epithelial cells [44]. Conversely, in mouse macrophages, this mechanism was prevented in a negative feedback loop by which p65/p52 triggers a hyperactive NfκbIa promoter, causing late IκBa production and reducing late p65/p50 and RelA/p52 activities, thus limiting the negative effects of prolonged macrophage triggering [45]. Our findings suggest that disruptions in cell type-specific control of NF-κB cross-talks, resulting in sustained p65/p52 nuclear activity, may contribute to the pro-tumoral behavior of TAMs, thus opening new directions to approach TAMs reprogramming through NF-κB modulation.

Despite the general inherent limitations of molecular investigations and the need for a major understanding of the physiological role of NF-κB pathways crosstalk, our results unveil the first evidence of unexplored p65/p52 dimer activity in TAMs.

This novel molecular target, along with identified regulatory regions on known genes impacting macrophage behavior and tumor biology, might now be exploited to develop novel targeted therapeutic strategies aimed at modulating TAMs functions towards anti-tumoral phenotypes, improving cancer treatment outcomes.

Funding

This research was funded by Regione Lazio, LAZIO INNOVA (A0375-2020-36621) to C.P.

CRediT authorship contribution statement

Veronica De Paolis: Writing – review & editing, Writing – original draft, Visualization, Validation, Software, Methodology, Investigation, Formal analysis, Data curation, Conceptualization. **Virginia Troisi:** Methodology, Data curation. **Antonella Bordin:** Software. **Francesca Pagano:** Writing – review & editing. **Viviana Caputo:** Writing – review & editing, Writing – original draft. **Chiara Parisi:** Writing – review & editing, Writing – original draft, Visualization, Validation, Supervision, Resources, Project administration, Investigation, Funding acquisition, Conceptualization.

Declaration of competing interest

The authors declare that they have no known competing financial interests or personal relationships that could have appeared to influence the work reported in this paper.

Data availability statement

All relevant data presented in this study are included in the article and its supplementary information files. Any other data that support the findings discussed here are available from the corresponding author upon request.

Acknowledgments

Veronica De Paolis was supported by Fondazione Umberto Veronesi.

Appendix A. Supplementary data

Supplementary data to this article can be found online at https://doi.org/10.1016/j.lfs.2024.123059.

References

[1] R.L. Siegel, A.N. Giaquinto, A. Jemal, Cancer statistics, CA A Cancer J Clinicians 74 (2024) (2024) 12–49, https://doi.org/10.3322/caac.21820.
[2] A. Baranova, Department of Radiology and Oncology, Grigoriev Institute for Medical Radiology NAMS of Ukraine, Kharkiv, Ukraine, Department of Oncology, Kharkiv National Medical University, Kharkiv, Ukraine. Triple-negative breast cancer: current treatment strategies and factors of negative prognosis, JMedLife 15 (2022) 153–161, https://doi.org/10.25122/jml-2021-0108.
[3] F. Font-Clos, S. Zapperi, C.A.M. La Porta, Classification of triple negative breast cancer by epithelial mesenchymal transition and the tumor immune microenvironment, Sci. Rep. 12 (2022) 9651, https://doi.org/10.1038/s41598-022-13428-2.
[4] K.G.K. Deepak, R. Vempati, G.P. Nagaraju, V.R. Dasari, N. S., D.N. Rao, R.R. Malla, Tumor microenvironment: challenges and opportunities in targeting metastasis of triple negative breast cancer, Pharmacol. Res. 153 (2020) 104683. https://doi.org/10.1016/j.phrs.2020.104683.
[5] S. Loizides, A. Constantinidou, Triple negative breast cancer: immunogenicity, tumor microenvironment, and immunotherapy, Front. Genet. 13 (2023) 1095839, https://doi.org/10.3389/fgene.2022.1095839.
[6] Z. Yuan, Y. Li, S. Zhang, X. Wang, H. Dou, X. Yu, Z. Zhang, S. Yang, M. Xiao, Extracellular matrix remodeling in tumor progression and immune escape: from mechanisms to treatments, Mol. Cancer 22 (2023) 48, https://doi.org/10.1186/s12943-023-01744-8.
[7] L. Cao, X. Meng, Z. Zhang, Z. Liu, Y. He, Macrophage heterogeneity and its interactions with stromal cells in tumour microenvironment, Cell Biosci. 14 (2024) 16, https://doi.org/10.1186/s13578-024-01201-z.
[8] L. Cassetta, J.W. Pollard, A timeline of tumour-associated macrophage biology, Nat. Rev. Cancer 23 (2023) 238–257, https://doi.org/10.1038/s41568-022-00547-1.
[9] A.K. Mehta, S. Kadel, M.G. Townsend, M. Oliwa, J.L. Guerriero, Macrophage biology and mechanisms of immune suppression in breast Cancer, Front. Immunol. 12 (2021) 643771, https://doi.org/10.3389/fimmu.2021.643771.
[10] K.Y. Jung, S.W. Cho, Y.A. Kim, D. Kim, B.-C. Oh, D.J. Park, Y.J. Park, Cancers with higher density of tumor-associated macrophages were associated with poor survival rates, J. Pathol. Transl. Med. 49 (2015) 318–324, https://doi.org/10.4132/jptm.2015.06.01.
[11] L. Xu, X. Xie, Y. Luo, The role of macrophage in regulating tumour microenvironment and the strategies for reprogramming tumour-associated macrophages in antitumour therapy, Eur. J. Cell Biol. 100 (2021) 151153, https://doi.org/10.1016/j.ejcb.2021.151153.
[12] A. Mantovani, P. Allavena, F. Marchesi, C. Garlanda, Macrophages as tools and targets in cancer therapy, Nat. Rev. Drug Discov. 21 (2022) 799–820, https://doi.org/10.1038/s41573-022-00520-5.
[13] J. Cornice, D. Verzella, P. Arboretto, D. Vecchiotti, D. Capece, F. Zazzeroni, G. Franzoso, NF-κB: governing macrophages in Cancer, Genes 15 (2024) 197, https://doi.org/10.3390/genes15020197.
[14] A. Hoffmann, G. Natoli, G. Ghosh, Transcriptional regulation via the NF-κB signaling module, Oncogene 25 (2006) 6706–6716, https://doi.org/10.1038/sj.onc.1209933.
[15] A. Oeckinghaus, S. Ghosh, The NF- B family of transcription factors and its regulation, Cold Spring Harb. Perspect. Biol. 1 (2009) a000034, https://doi.org/10.1101/cshperspect.a000034.
[16] D. Wong, A. Teixeira, S. Oikonomopoulos, P. Humburg, I. Lone, D. Saliba, T. Siggers, M. Bulyk, D. Angelov, S. Dimitrov, I.A. Udalova, J. Ragoussis, Extensive characterization of NF-κB binding uncovers non-canonical motifs and advances the interpretation of genetic functional traits, Genome Biol. 12 (2011) R70, https://doi.org/10.1186/gb-2011-12-7-r70.
[17] M. Hinz, C. Scheidereit, The IκB kinase complex in NF -κB regulation and beyond, EMBO Rep. 15 (2014) 46–61, https://doi.org/10.1002/embr.201337983.
[18] P. Collins, I. Mitxitorena, R. Carmody, The ubiquitination of NF-κB subunits in the control of transcription, Cells 5 (2016) 23, https://doi.org/10.3390/cells5020023.
[19] J. Napetschnig, H. Wu, Molecular basis of NF-κB signaling, Annu. Rev. Biophys. 42 (2013) 443–468, https://doi.org/10.1146/annurev-biophys-083012-130338.
[20] M.S. Hayden, S. Ghosh, Shared principles in NF-κB signaling, Cell 132 (2008) 344–362, https://doi.org/10.1016/j.cell.2008.01.020.
[21] S.-C. Sun, Non-canonical NF-κB signaling pathway, Cell Res. 21 (2011) 71–85, https://doi.org/10.1038/cr.2010.177.

[22] M. Devanaboyina, J. Kaur, E. Whiteley, L. Lin, K. Einloth, S. Morand, L. Stanbery, D. Hamouda, J. Nemunaitis, NF-κB signaling in tumor pathways focusing on breast and ovarian Cancer, Oncol. Rev. 16 (2022) 10568, https://doi.org/10.3389/or.2022.10568.
[23] R. He, Y. He, R. Du, C. Liu, Z. Chen, A. Zeng, L. Song, Revisiting of TAMs in tumor immune microenvironment: insight from NF-κB signaling pathway, Biomed. Pharmacother. 165 (2023) 115090, https://doi.org/10.1016/j.biopha.2023.115090.
[24] R.R. Malla, P. Kiran, Tumor microenvironment pathways: cross regulation in breast cancer metastasis, Genes & Diseases 9 (2022) 310–324, https://doi.org/10.1016/j.gendis.2020.11.015.
[25] E. Pavitra, J. Kancharla, V.K. Gupta, K. Prasad, J.Y. Sung, J. Kim, M.B. Tej, R. Choi, J.-H. Lee, Y.-K. Han, G.S.R. Raju, L. Bhaskar, Y.S. Huh, The role of NF-κB in breast cancer initiation, growth, metastasis, and resistance to chemotherapy, Biomed. Pharmacother. 163 (2023) 114822, https://doi.org/10.1016/j.biopha.2023.114822.
[26] N.D. Mineva, X. Wang, S. Yang, H. Ying, Z.J. Xiao, M.F. Holick, G.E. Sonenshein, Inhibition of RelB by 1,25-dihydroxyvitamin D $_3$ promotes sensitivity of breast cancer cells to radiation, journal cellular, Physiology 220 (2009) 593–599, https://doi.org/10.1002/jcp.21765.
[27] H.-Y. Tan, N. Wang, K. Man, S.-W. Tsao, C.-M. Che, Y. Feng, Autophagy-induced RelB/p52 activation mediates tumour-associated macrophage repolarisation and suppression of hepatocellular carcinoma by natural compound baicalin, Cell Death Dis. 6 (2015) e1942, https://doi.org/10.1038/cddis.2015.271.
[28] Y. Yu, Y. Wan, C. Huang, The Biological Functions of NF-κB1 (p) and its Potential as an Anti-Cancer Target, CCDT 9 (2009) 566–571. https://doi.org/10.2174/156800909788486759.
[29] A. Saccani, T. Schioppa, C. Porta, S.K. Biswas, M. Nebuloni, L. Vago, B. Bottazzi, M. P. Colombo, A. Mantovani, A. Sica, p50 nuclear factor-kappaB overexpression in tumor-associated macrophages inhibits M1 inflammatory responses and antitumor resistance, Cancer Res. 66 (2006) 11432–11440, https://doi.org/10.1158/0008-5472.CAN-06-1867.
[30] V. De Paolis, F. Maiullari, M. Chirivì, M. Milan, C. Cordiglieri, F. Pagano, A.R. La Manna, E. De Falco, C. Bearzi, R. Rizzi, C. Parisi, Unusual association of NF-κB components in tumor-associated macrophages (TAMs) promotes HSPG2-mediated immune-escaping mechanism in breast Cancer, IJMS 23 (2022) 7902, https://doi.org/10.3390/ijms23147902.
[31] P. Schober, C. Boer, L.A. Schwarte, Correlation coefficients: appropriate use and interpretation, Anesth. Analg. 126 (2018) 1763–1768, https://doi.org/10.1213/ANE.0000000000002864.
[32] H. Yu, L. Lin, Z. Zhang, H. Zhang, H. Hu, Targeting NF-κB pathway for the therapy of diseases: mechanism and clinical study, Sig Transduct Target Ther 5 (2020) 209, https://doi.org/10.1038/s41392-020-00312-6.
[33] M. Baer, A. Dillner, R.C. Schwartz, C. Sedon, S. Nedospasov, P.F. Johnson, Tumor necrosis factor alpha transcription in macrophages is attenuated by an autocrine factor that preferentially induces NF-κB p50, Mol. Cell. Biol. 18 (1998) 5678–5689, https://doi.org/10.1128/MCB.18.10.5678.
[34] K.R. Rosenbloom, C.A. Sloan, V.S. Malladi, T.R. Dreszer, K. Learned, V.M. Kirkup, M.C. Wong, M. Maddren, R. Fang, S.G. Heitner, B.T. Lee, G.P. Barber, R.A. Harte, M. Diekhans, J.C. Long, S.P. Wilder, A.S. Zweig, D. Karolchik, R.M. Kuhn, D. Haussler, W.J. Kent, ENCODE data in the UCSC genome browser: year 5 update, Nucleic Acids Res. 41 (2012) D56–D63, https://doi.org/10.1093/nar/gks1172.
[35] J.A. Castro-Mondragon, R. Riudavets-Puig, I. Rauluseviciute, R. Berhanu Lemma, L. Turchi, R. Blanc-Mathieu, J. Lucas, P. Boddie, A. Khan, N. Manosalva Pérez, O. Fornes, T.Y. Leung, A. Aguirre, F. Hammal, D. Schmelter, D. Baranasic, B. Ballester, A. Sandelin, B. Lenhard, K. Vandepoele, W.W. Wasserman, F. Parcy, A. Mathelier, JASPAR 2022: The 9th release of the open-access database of transcription factor binding profiles, Nucleic Acids Res. 50 (2022) D165–D173. https://doi.org/10.1093/nar/gkab1113.
[36] F. Hammal, P. de Langen, A. Bergon, F. Lopez, B. Ballester, ReMap 2022: A database of human, mouse, Drosophila and Arabidopsis regulatory regions from an integrative analysis of DNA-binding sequencing experiments, Nucleic Acids Res. 50 (2022) D316–D325. https://doi.org/10.1093/nar/gkab996.
[37] C.R. Warren, B.J. Grindel, L. Francis, D.D. Carson, M.C. Farach-Carson, Transcriptional activation by NFκB increases perlecan/HSPG2 expression in the desmoplastic prostate tumor microenvironment, J. Cell. Biochem. 115 (2014) 1322–1333, https://doi.org/10.1002/jcb.24788.
[38] M. Tegowski, A. Baldwin, Noncanonical NF-κB in Cancer, Biomedicines 6 (2018) 66, https://doi.org/10.3390/biomedicines6020066.
[39] X. Huang, J. Cao, X. Zu, Tumor-associated macrophages: an important player in breast cancer progression, thoracic, Cancer 13 (2022) 269–276, https://doi.org/10.1111/1759-7714.14268.
[40] M. Mongiat, K. Taylor, J. Otto, S. Aho, J. Uitto, J.M. Whitelock, R.V. Iozzo, The protein core of the proteoglycan perlecan binds specifically to fibroblast growth factor-7, J. Biol. Chem. 275 (2000) 7095–7100, https://doi.org/10.1074/jbc.275.10.7095.
[41] J.A. Hamilton, A. Achuthan, Colony stimulating factors and myeloid cell biology in health and disease, Trends Immunol. 34 (2013) 81–89, https://doi.org/10.1016/j.it.2012.08.006.
[42] A.A. Barkal, K. Weiskopf, K.S. Kao, S.R. Gordon, B. Rosental, Y.Y. Yiu, B.M. George, M. Markovic, N.G. Ring, J.M. Tsai, K.M. McKenna, P.Y. Ho, R.Z. Cheng, J.Y. Chen, L.J. Barkal, A.M. Ring, I.L. Weissman, R.L. Maute, Engagement of MHC class I by the inhibitory receptor LILRB1 suppresses macrophages and is a target of cancer immunotherapy, Nat. Immunol. 19 (2018) 76–84, https://doi.org/10.1038/s41590-017-0004-z.
[43] K. Ganesh, J. Massagué, TGF-β inhibition and immunotherapy: checkmate, Immunity 48 (2018) 626–628, https://doi.org/10.1016/j.immuni.2018.03.037.
[44] B. Banoth, B. Chatterjee, B. Vijayaragavan, M. Prasad, P. Roy, S. Basak, Stimulus-selective crosstalk via the NF-κB signaling system reinforces innate immune response to alleviate gut infection, eLife 4 (2015) e05648. https://doi.org/10.7554/eLife.05648.
[45] B. Chatterjee, B. Banoth, T. Mukherjee, N. Taye, B. Vijayaragavan, S. Chattopadhyay, J. Gomes, S. Basak, Late-phase synthesis of IκBα insulates the TLR4-activated canonical NF-κB pathway from noncanonical NF-κB signaling in macrophages, Sci. Signal. 9 (2016), https://doi.org/10.1126/scisignal.aaf1129.